SIM&TEC

Simulación y Tecnología

Simulation and Technology

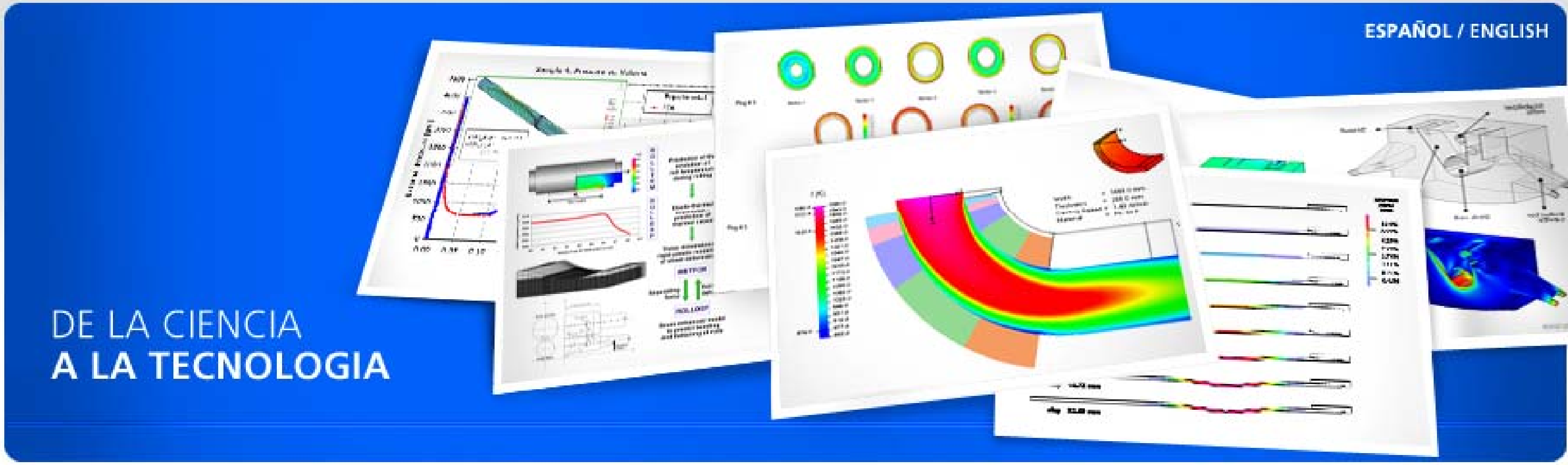

Advanced Topics in Computational Solid Mechanics. Industrial Applications

Section 10: Modeling of Steel Pipes Collapse: Industrial Examples

Eduardo N. Dvorkin

Stanford University
Mechanical Engineering
Winter Quarter 2010

Technological Problem

Deep Water Installations

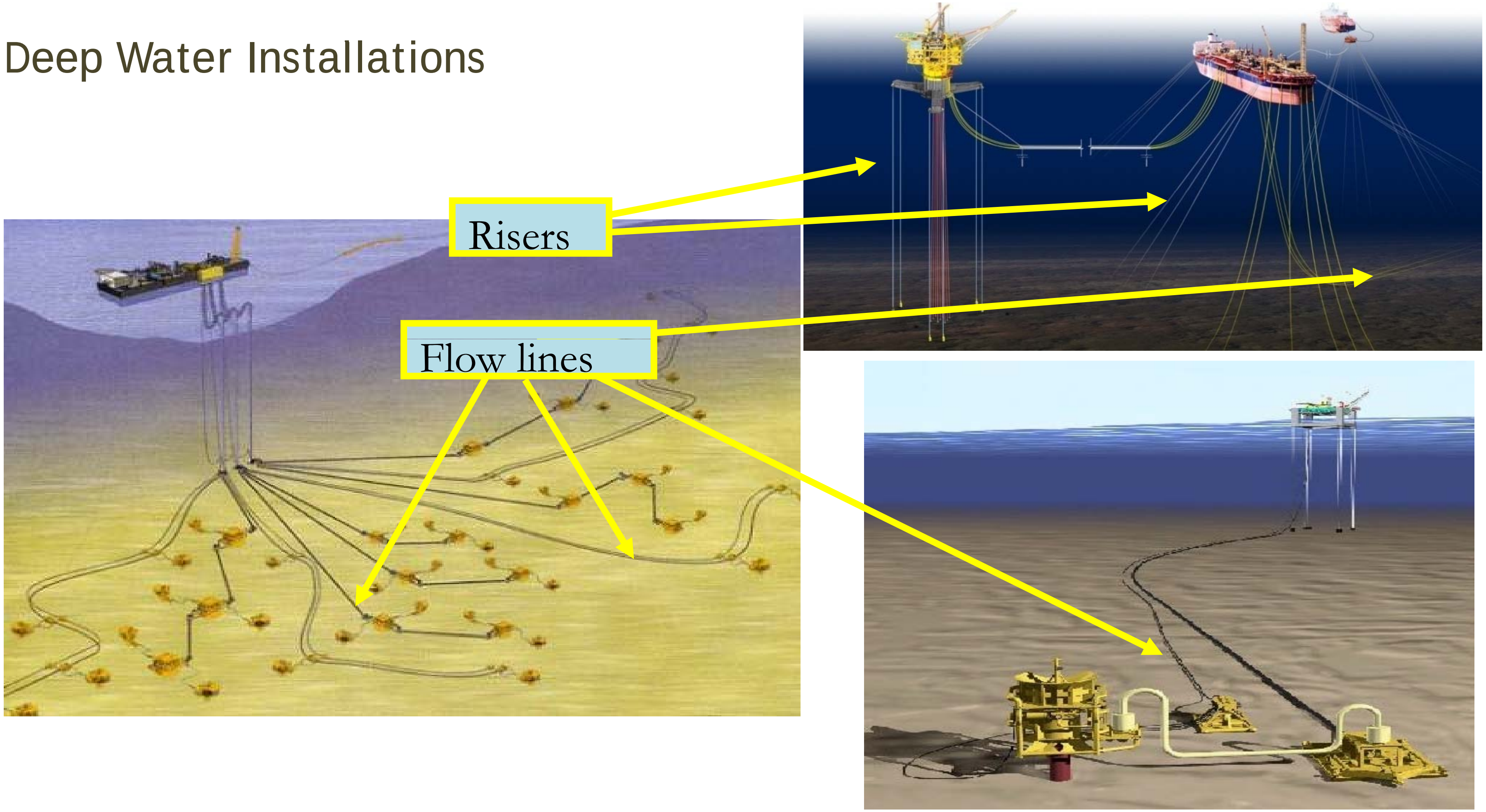

Construction Techniques

S-lay barge pipeling

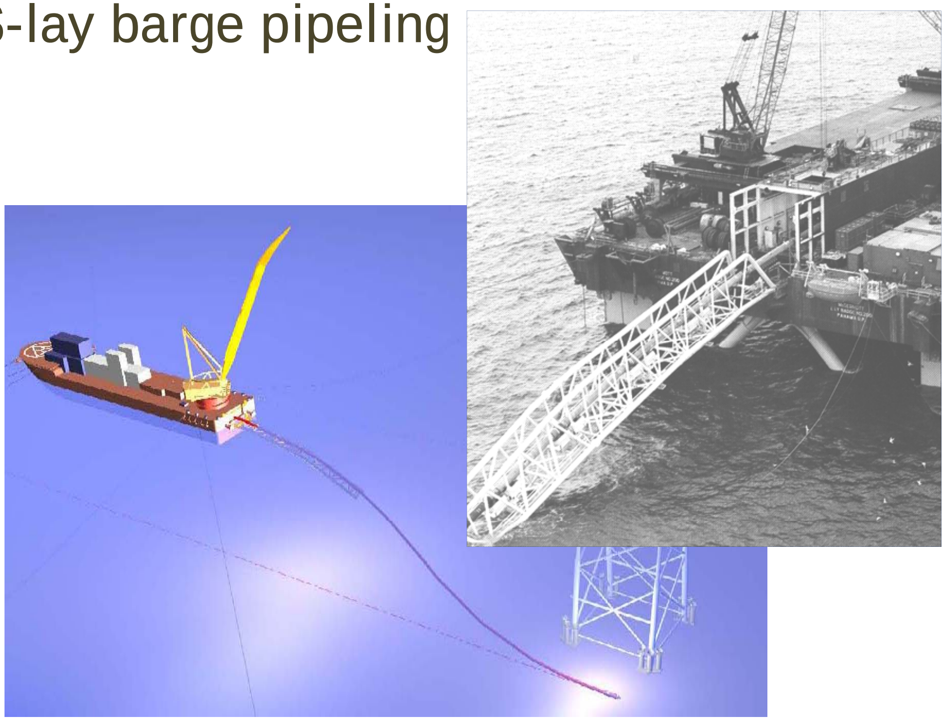

J-lay barge pipeling

- S-lay takes its name from the suspended shape of the pipe at the end of the barge, which lays in an elongated "S" from the stringer to the seabed.

- For the J-lay, the suspended pipe forms a "J" from the vessel to the seabed.

Construction Techniques

Reel-lay barge pipeling

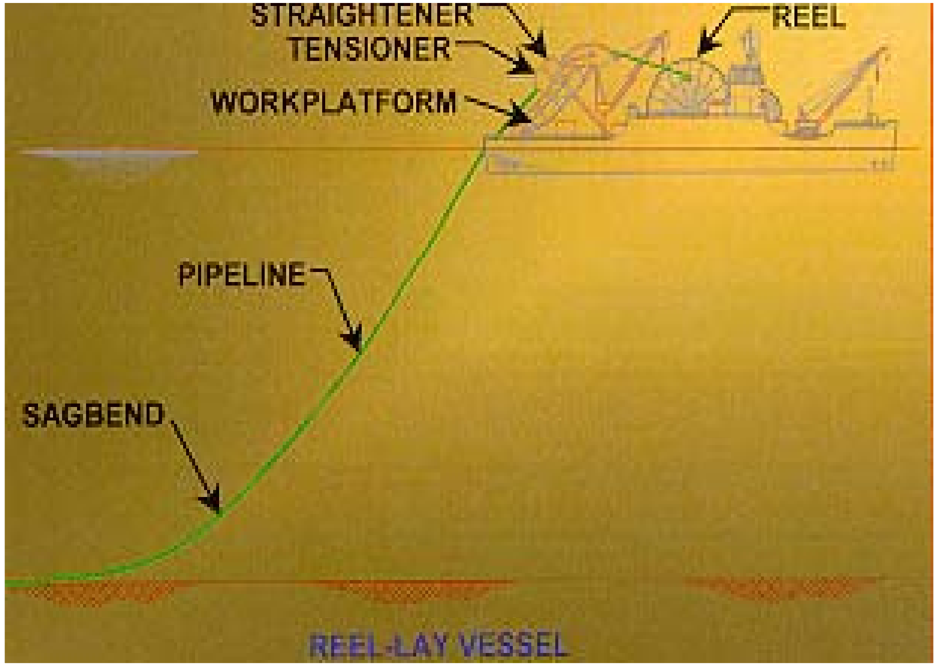

Reel-lay method: the pipe is assembled onshore and wound onto a large reel on the vessel; before to be J-laid on its final location it has to be unwound and straightened.

Failure Modes

- Global buckling

(buckling of the pipe as a bar in compression → column mode)

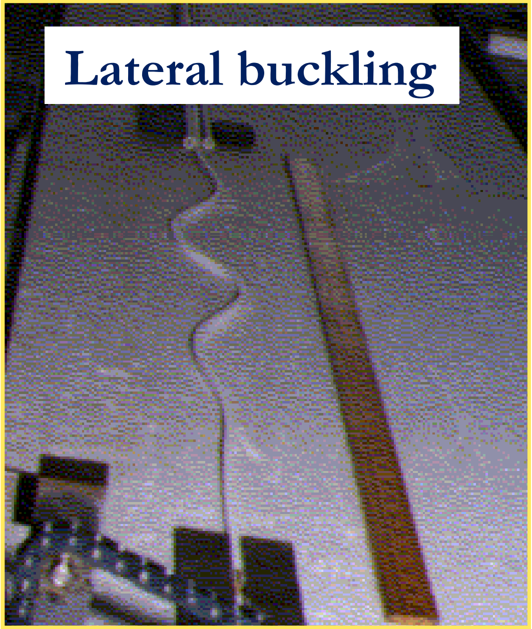

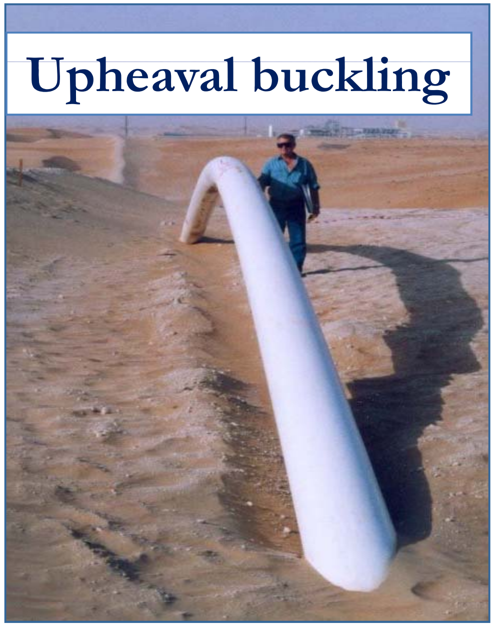

Internal pressure → Destabilizing effect

Palmer A.C. (1974), "Lateral Buckling of Axially Constrained Pipelines"
Dvorkin E.N. and Toscano R.G. (2001), "Effects of external/internal pressure on the global buckling of pipelines".

Failure Modes

- Local buckling

Structural collapse of steel tubes under external pressure

Buckle Arrestor

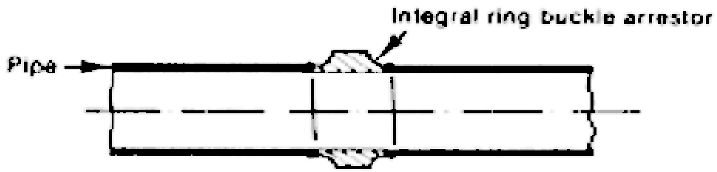

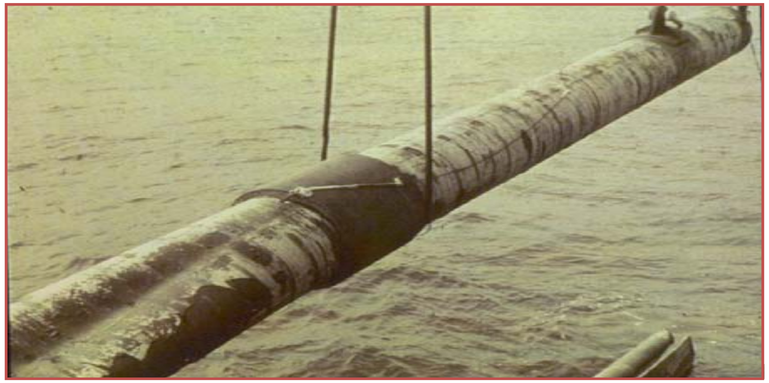

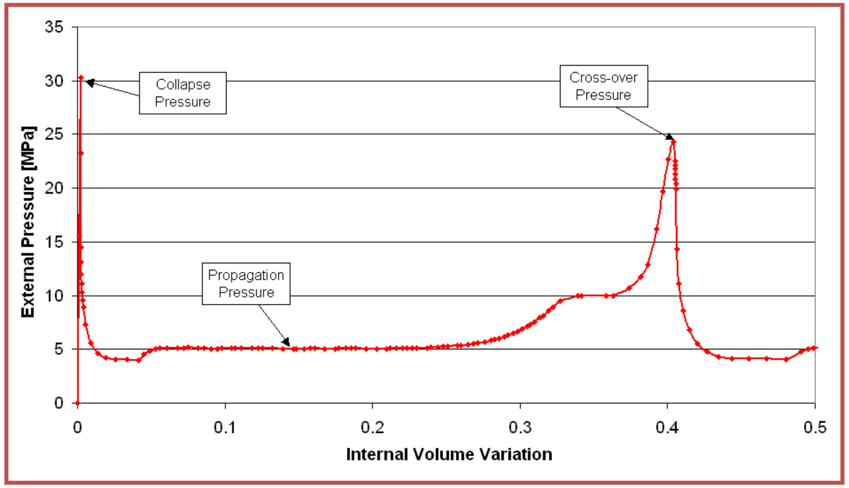

Collapse propagation pressure: The lowest pressure which can sustain a propagation buckle *(Andrew Palmer)*

Crossover pressure : The minimum pressure value at which the buckle crosses over the arrestor

SIM&TEC
Simulación y Tecnología
Simulation and Technology

2D Continuum Mesh

Two dimensional finite element model of very long pipes

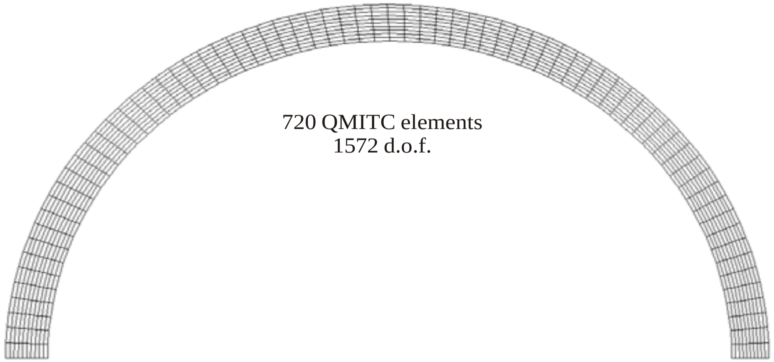

OD	245.42 mm
Wall thickness	12.61 mm
Ovality	0.18 %
Yield stress	890 MPa
Theoretical Pcr	64.36 MPa
$\dfrac{[p_{cr}]_{theoretical}}{[p_{cr}]_{2D}}$	0.992

Qualification of 2D continuum elements model , Rs=0. (*Timoshenko*)

- Total Lagrangian formulation.
- QMITC plane strain element (4-noded element) *(Dvorkin-Vassolo)*
- Automatic solution of the incremental nonlinear finite element equations (Riks method).
- Elasto-plastic material model: von Mises associated plasticity with isotropic hardening.
- Geometrical nonlinearity: large displacements / rotations but small strains.
- ADINA code (special version)
- Follower loads
- Residual stresses: linear distribution trough the thickness

2D Continuum Mesh

Parametric analyses

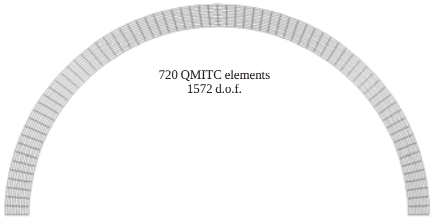

$$Ov(\%) = \frac{(D_{max} - D_{min})}{D_{average}} \cdot 100$$

$$Ecc(\%) = \frac{(t_{max} - t_{min})}{t_{average}} \cdot 100$$

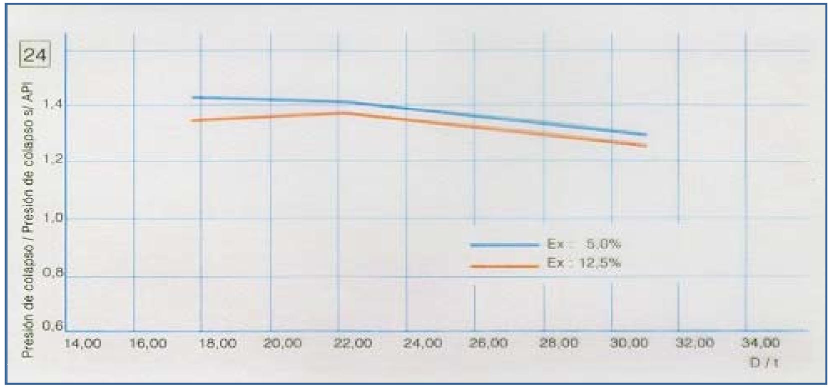

Eccentricity effect

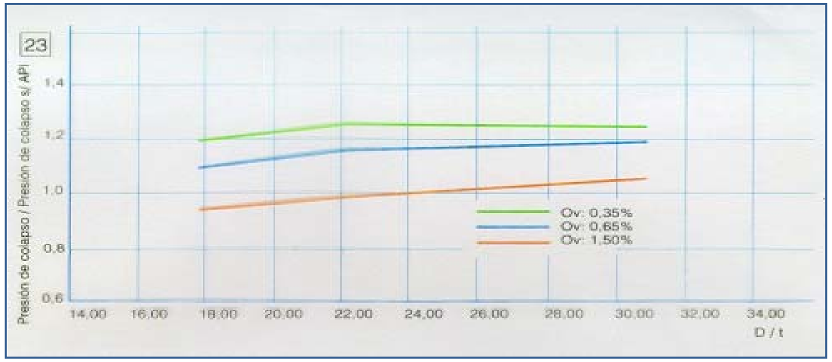

Ovality effect

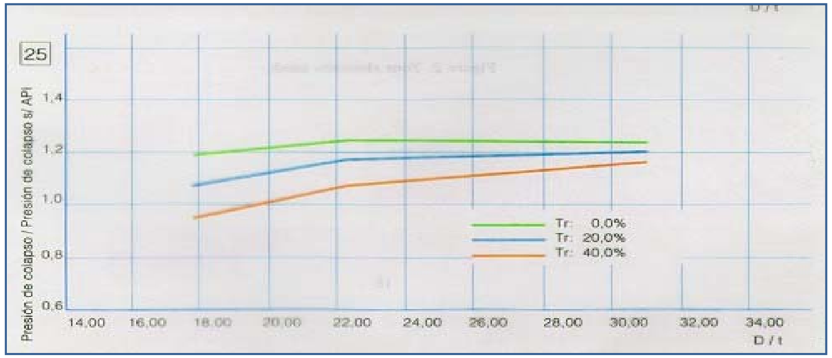

Residual stress effect

3D Finite Element of the Collapse and Post- collapse of very long pipes under Bending + external Pressure

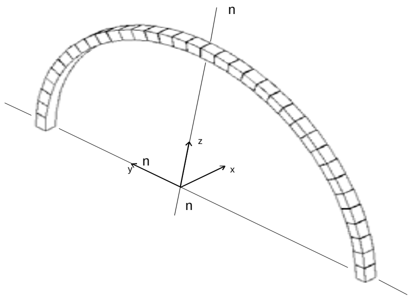

pipe central slice

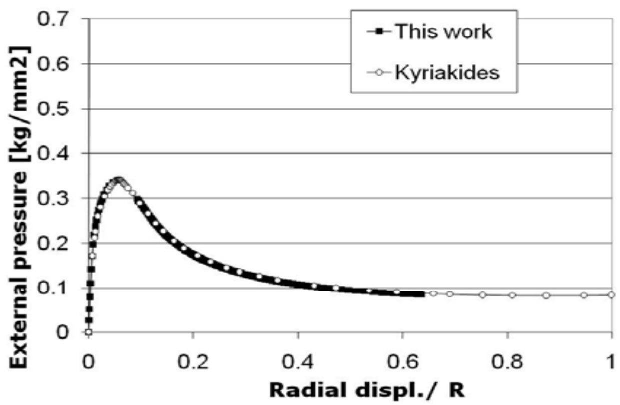

D=1.2522”
D/t=35
Sy=31.5 kg/mm2
E/Sy=225
E/Et = 86.5
Ov = 1.6%

- MITC4 shell element (4-noded element that includes shear deformation) *(Dvorkin and Bathe)*
- Automatic solution of the incremental nonlinear finite element equations. .
- Elasto-plastic material model: von Mises associated plasticity with isotropic hardening.
- Geometrical nonlinearity: large displacements / rotations but small strains.
- ADINA code
- Follower loads
- Residual stresses: linear distribution trough the thickness

3D Finite Element Model of very long pipes

8 5/8” OD 12.7# X60

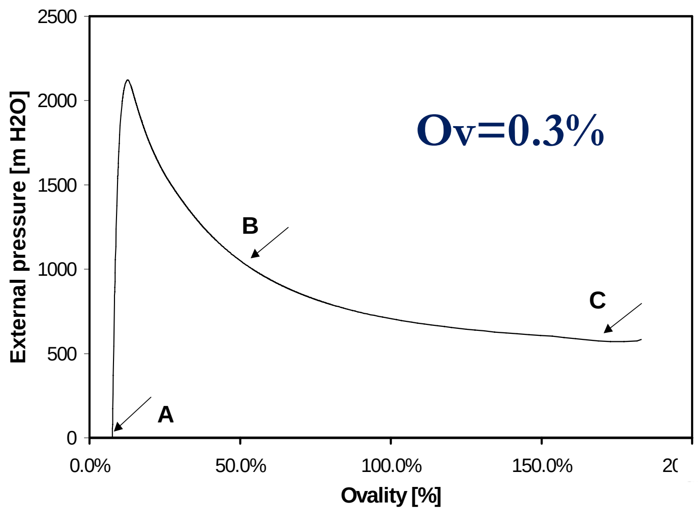

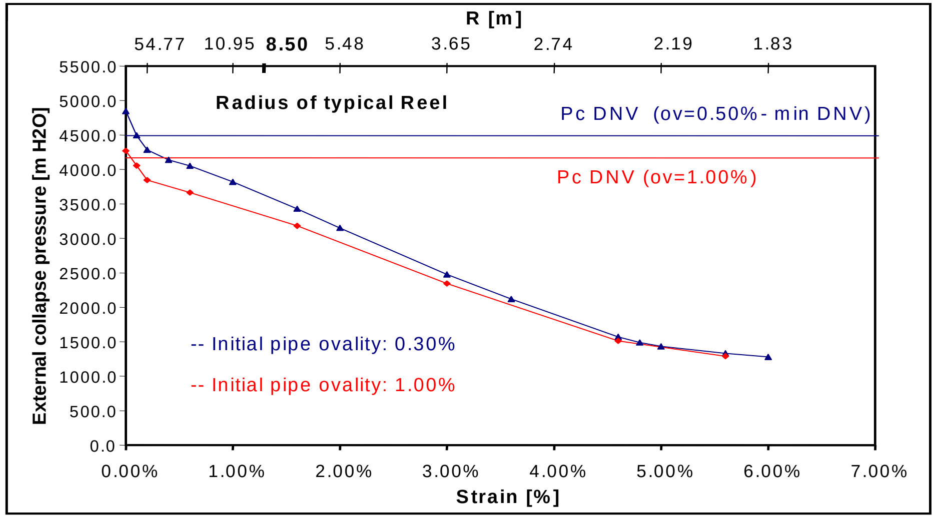

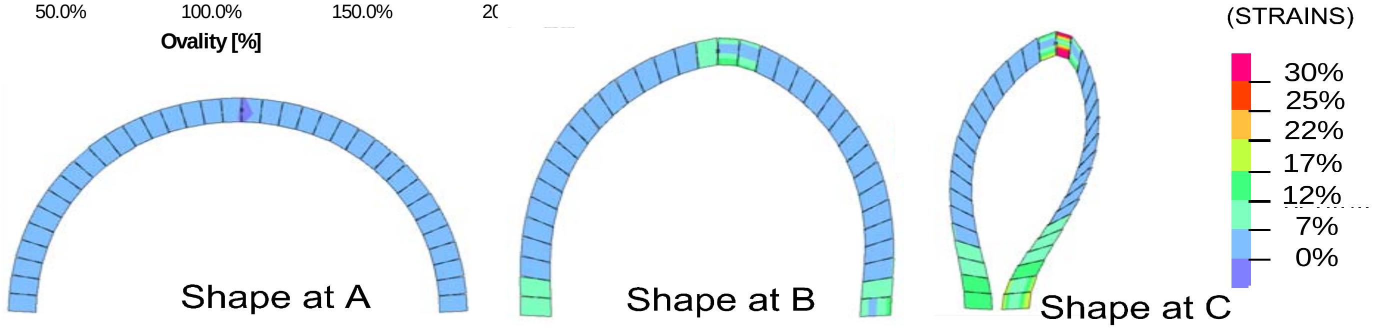

Initial, intermediate and final shapes of the pipe cross section
Equivalent logarithmic strains

3D Finite Element Simulation of the Slit- ring Test (industrial standard test)

9 5/8" OD 47 lb/ft P110

σ_R=0.2 σ_y

$$\sigma_R = \frac{a \cdot t \cdot E}{4 \cdot \pi \cdot R^2 \cdot (1-\nu^2)}$$ Long samples

$$\sigma_R = \frac{a \cdot t \cdot E}{4 \cdot \pi \cdot R^2}$$ Short samples

Sample length	a_{FEA} / $a_{analytical}$
25 mm	1.02
3D	0.99

a (opening)

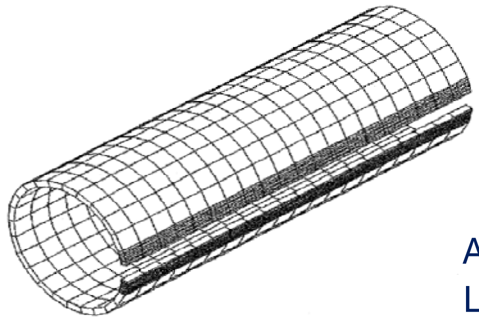

After slitting.
Lateral view.

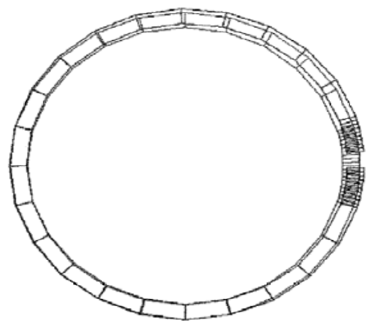

Before and after slitting. Front view.

Test specimens

Sample Number	Specimen Number	Average Measured OD (mm)	Average Measured t (mm)	OD/t	Maximum Ovality *	Maximum Eccentricity *	Test Type
1	7782	353.1	22.07	16.0	0.39	0.053	Collapse
2	7784	352.9	22.04	16.0	0.40	0.050	P→B
3	7871	353.0	21.84	16.2	0.41	0.069	P→B
4	7549	325.0	18.37	17.7	0.20	0.097	Collapse
5	7673	325.0	18.32	17.7	0.17	0.067	P→B
6	7548	325.2	18.18	17.9	0.21	0.051	P→B
7	7550	323.4	21.17	15.3	0.23	0.066	Collapse
8	7672	323.7	21.11	15.3	0.25	0.088	P→B
9	7547	323.8	21.14	15.3	0.20	0.081	B→P

Ovality=(OD_max.-OD_min.)/OD_av.

Eccentricity=(t_max.-t_min.)/t_nominal

Collapse and Propagation Tests

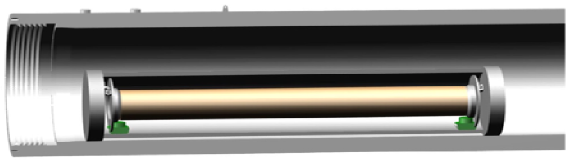

Combined Pressure and Bending Set-up

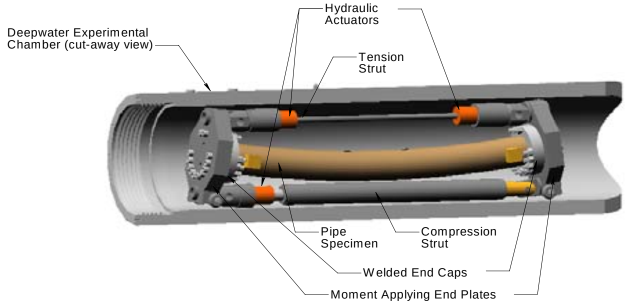

C-FER Technologies

Acquisition of the OD “shape”

(IMS, Imperfection Measuring System or “ shapemeter”)

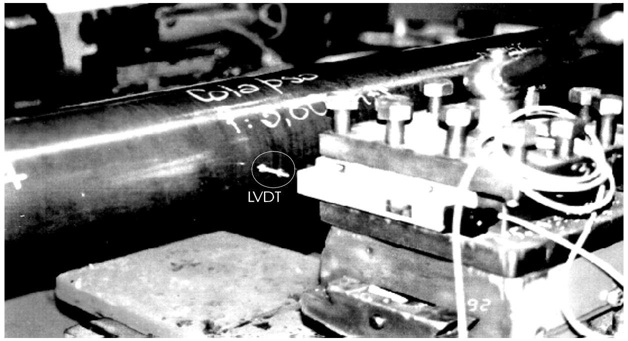

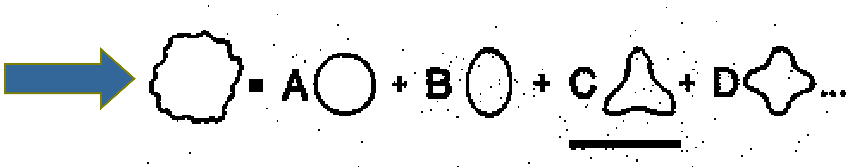

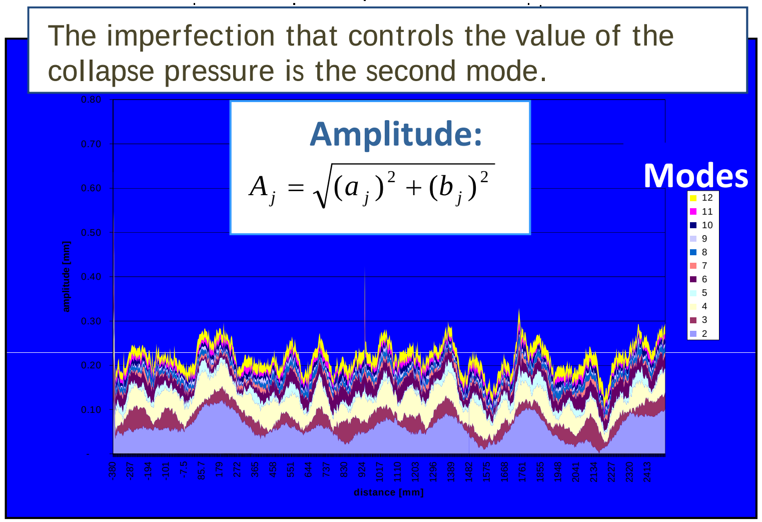

Algorithm to process the data acquired with the LVDT

Each specimen was divided in sections located a few millimeters apart. For each section, the circle that best fits the section’s outer surface was determined. Using the best-fit circle center, any point on the outer surface can be located with a radius and an angle,

$$r(\theta) = R_o + \sum_{j=1}^{N} \left[a_j \cos(j\theta) + b_j \sin(j\theta) \right]$$

(R_o is the best-fit circle radius)

* Assanelli A.P., Toscano R.G., Johnson D. and Dvorkin E.N. (2000), "Experimental / numerical analysis of the collapse behavior of steel pipes“
Yeh and Kyriakides S ; Arbocz, J. and Babcock, C.D. ; Arbocz, J. and Williams, J.G.

Mapping of the wall thickness

The thickness of the samples was mapped using a standard ultrasonic gauge.

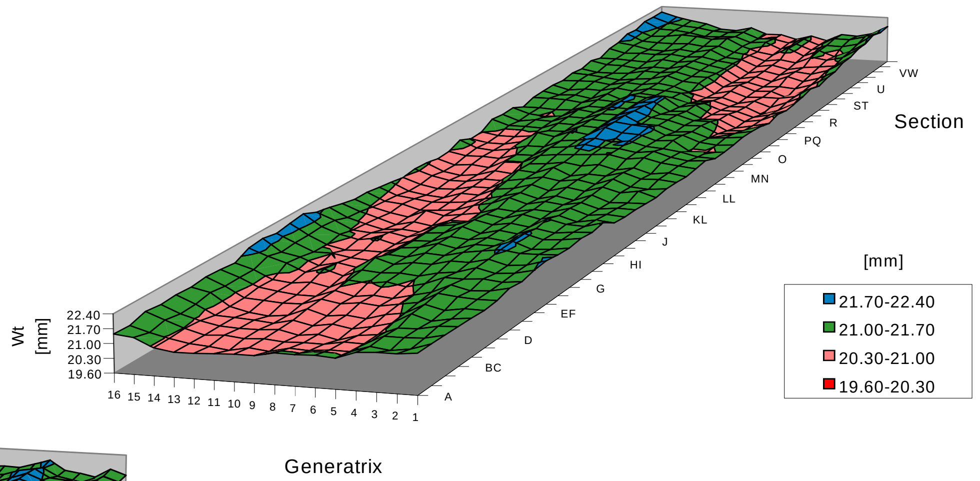

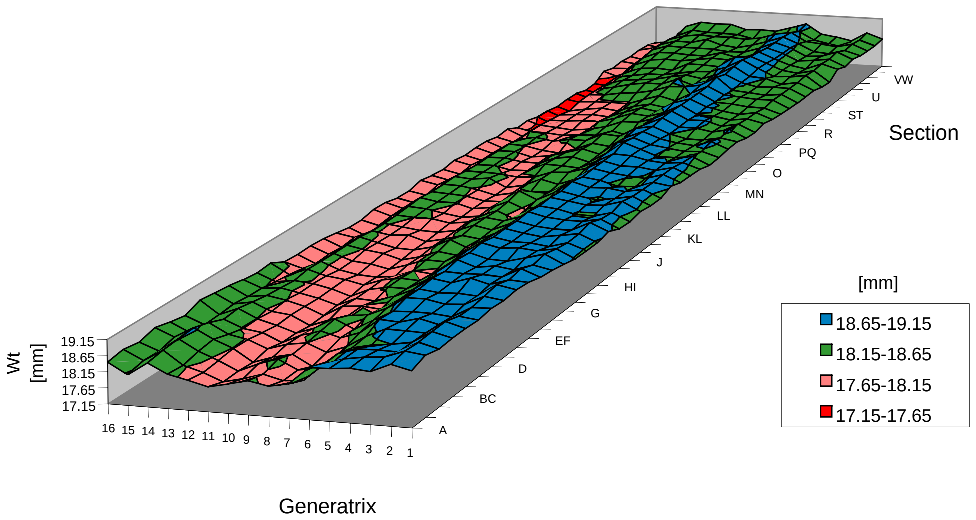

3D Finite Element Model

- MITC4 shell element (4-node element that includes shear deformation)
- ADINA code.
- Automatic solution of the incremental nonlinear finite element equations (Riks method).
- Elasto-plastic material model: von Mises associated plasticity with isotropic hardening, with the yield stress corresponding to the samples hoop yield stress in compression. In this model we neglect the plastic anisotropy of the material.
- Geometrical nonlinearity: large displacements / rotations but small strains.
- Contact elements on the pipe inner surface in order to prevent its inter-penetration in the post-collapse regime.
- Geometry described by the OD mapping and by the thickness distribution.
- Circumferential residual stresses obtained experimentally.

FST and FEA results for pipes under external pressure only. Pre and Post – collapse equilibrium paths

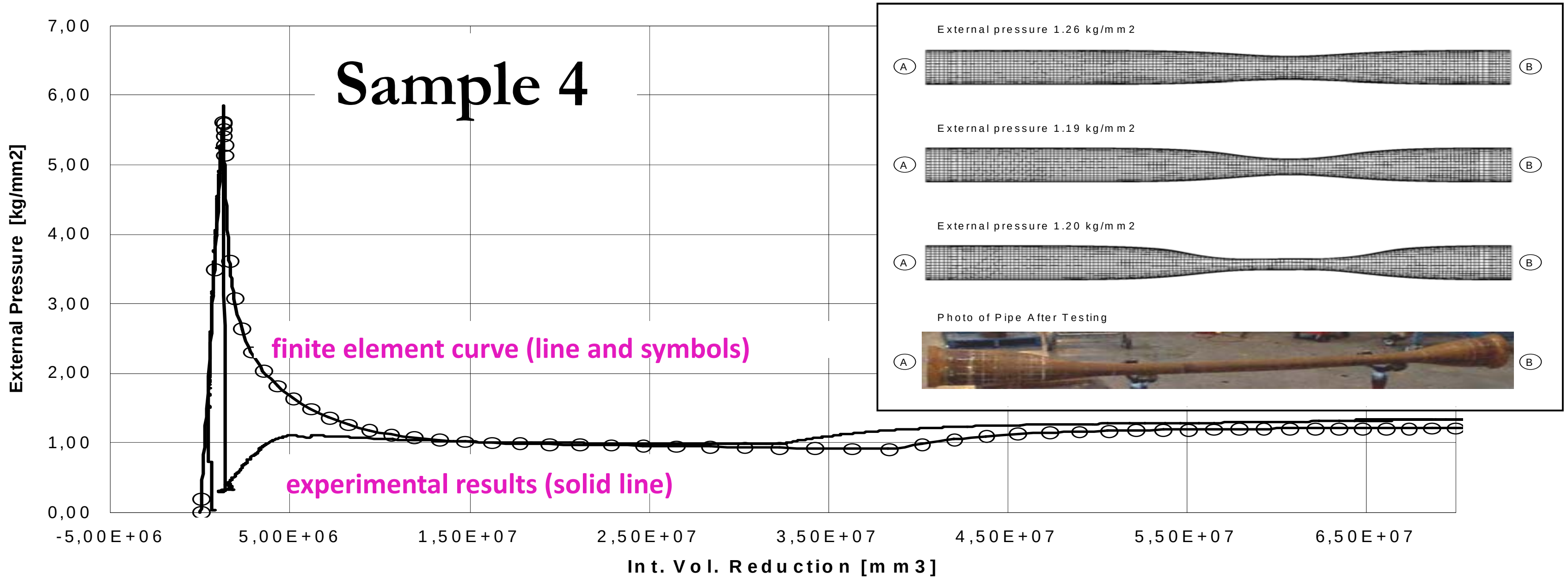

In the experimental test, after collapse the chamber is abruptly depressurized and water must be pumped to regain pressure. Hence, the experimental path is different from the numerical one, which better represents the undersea conditions.

FST and FEA results for Pressure Bend Tests

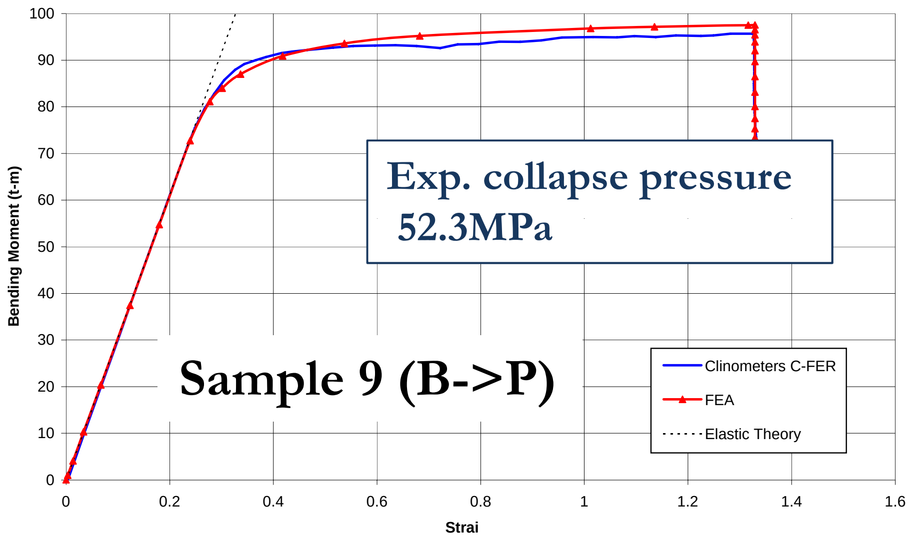

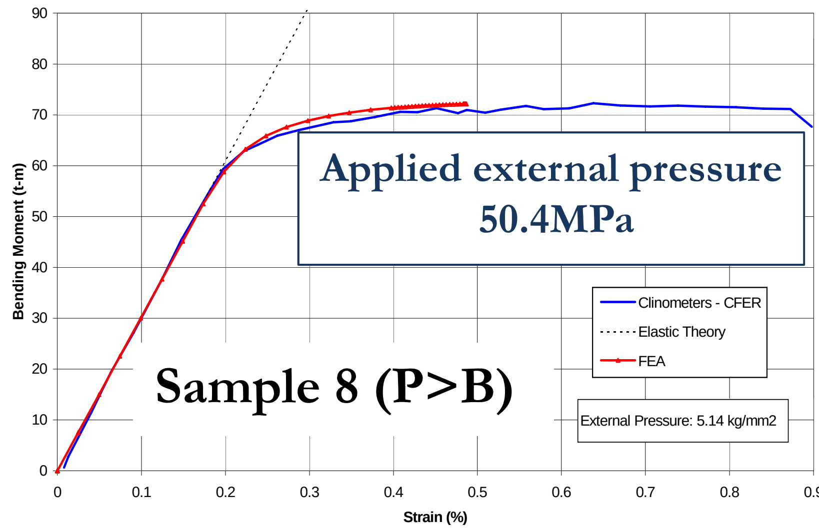

Bending moment vs. Average bending strain

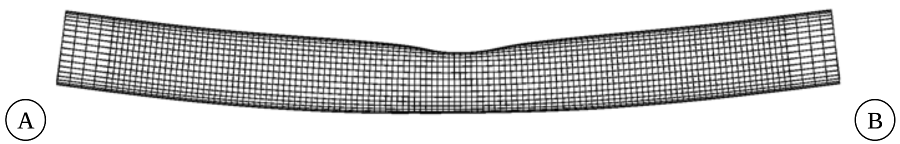

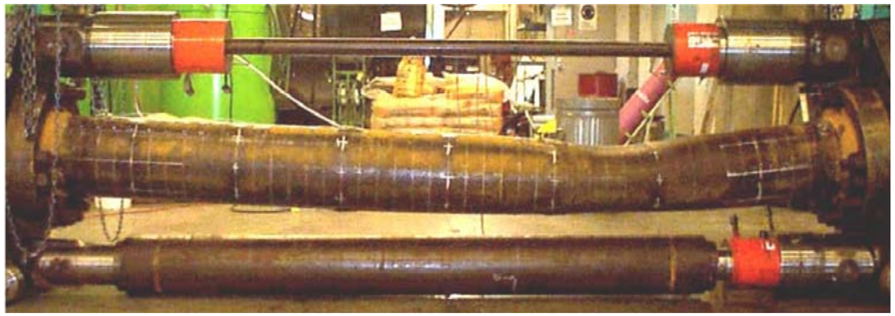

Summary: Numerical vs. Experimental Results

Sample	1	2	3	4	5	6	7	8	9
P_c FEA / P_c exp	0.977	--	--	0.966	--	--	1.103	--	0.964
Pprop FEA / Pprop exp	0.87	--	--	0.89	--	--	0.99	--	--
M_c FEA / M_c exp	--	1.047	1.088	--	0.972	0.998	--	0.998	--

The agreement between the finite element predictions and the laboratory observations, both in the pre- and post-collapse regimes is excellent; hence, the finite element models can be used as a reliable engineering tool for analyzing the effect of different imperfections, and of residual stresses, on the collapse and collapse propagation pressure of steel pipes.

Tested Samples

h=arrestor thickness
t= pipe thickness
La=arrestor length
D=pipe external diameter

Sample	Pipe OD [mm]	Pipe thickness (t) [mm]	Pipe steel grade	Arrestor (h/t)	Arrestor (La/D)	Arrestor steel grade	Sample length [mm]	Expected cross-over mechanism
1	141.3	6.55	X42	3.0	0.50	6 (ASTM A-333)	2240	Flattening
2	141.3	6.55	X42	2.5	0.50	X42	2250	Flattening
3	141.3	6.55	X42	3.0	0.75	X42	2274	Flipping
4	141.3	6.55	X42	3.0	1.00	X42	2330	Flipping

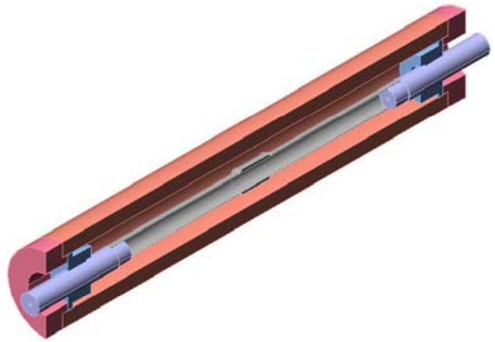

Tenaris Siderca lab.

flattening mode

flipping mode

*Kyriakides S., Park T.D. and Netto T.A.

Geometrical Measurements

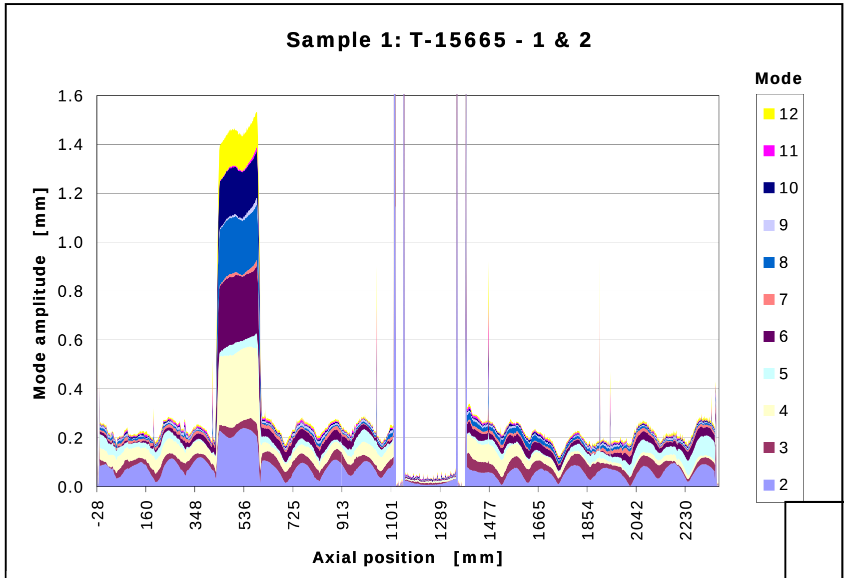

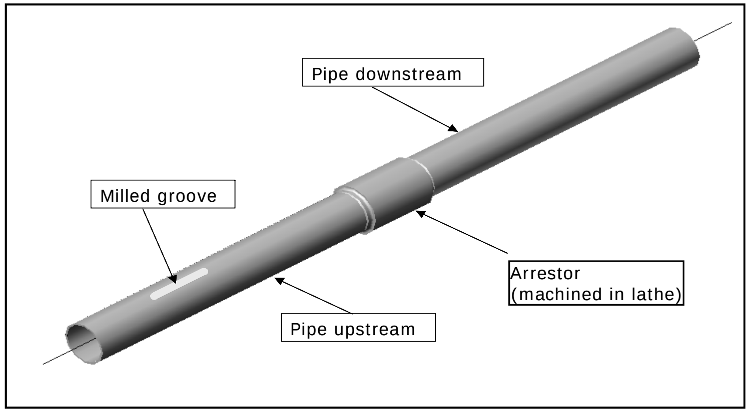

<u>OD Fourier Decomposition of a Pipe Specimen</u>:

Mode amplitude distribution as a function of the axial position along the sample.

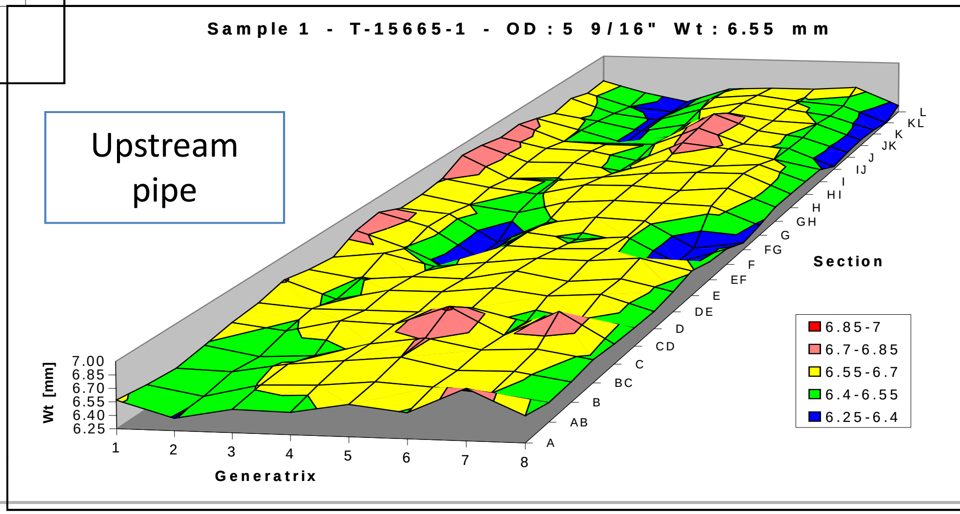

Thickness distribution (ultrasonic gauges)

Validation: Numerical vs. Experimental Response

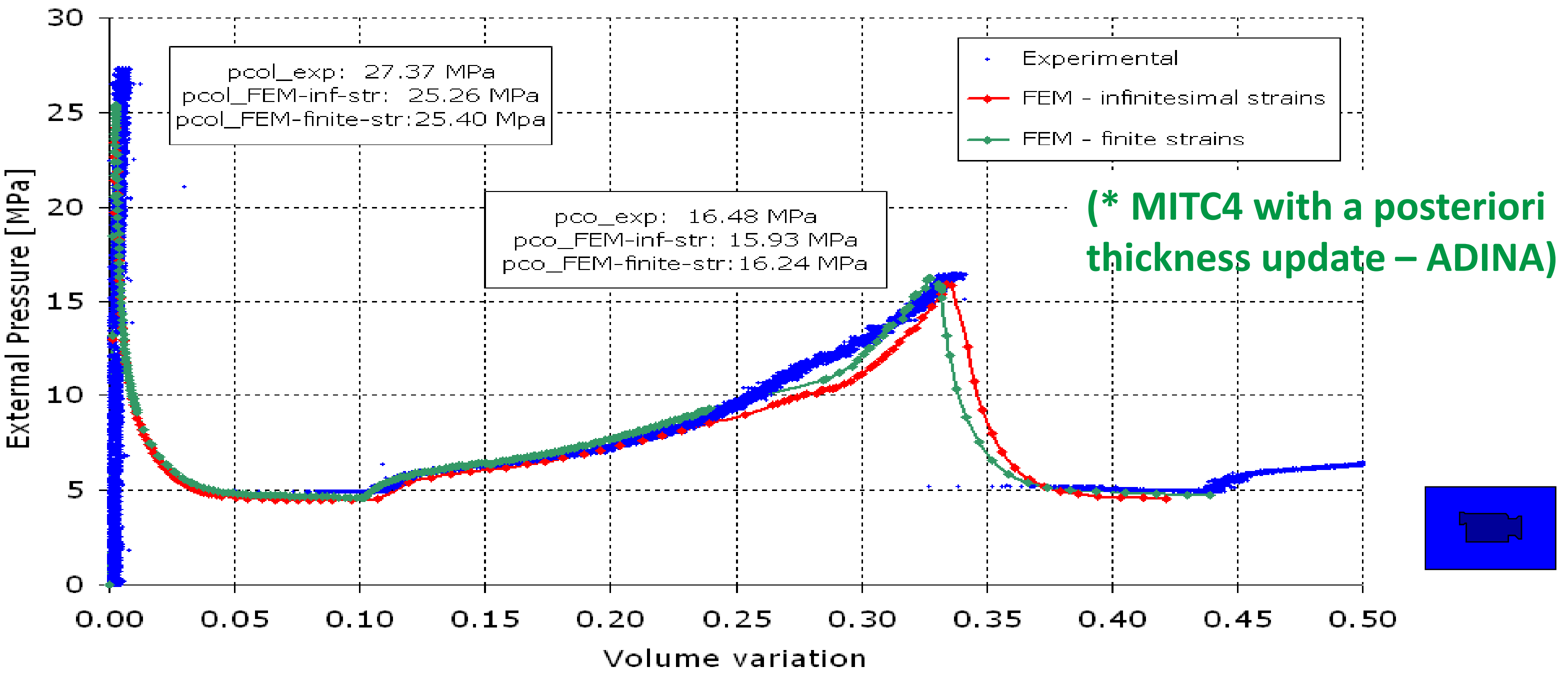

(* MITC4 with a posteriori thickness update – ADINA)

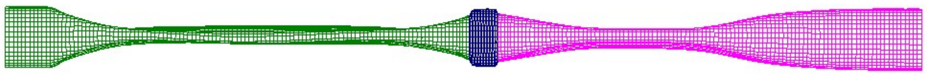

Validation: Numerical vs. Experimental Response

Infinitesimal or finite strains

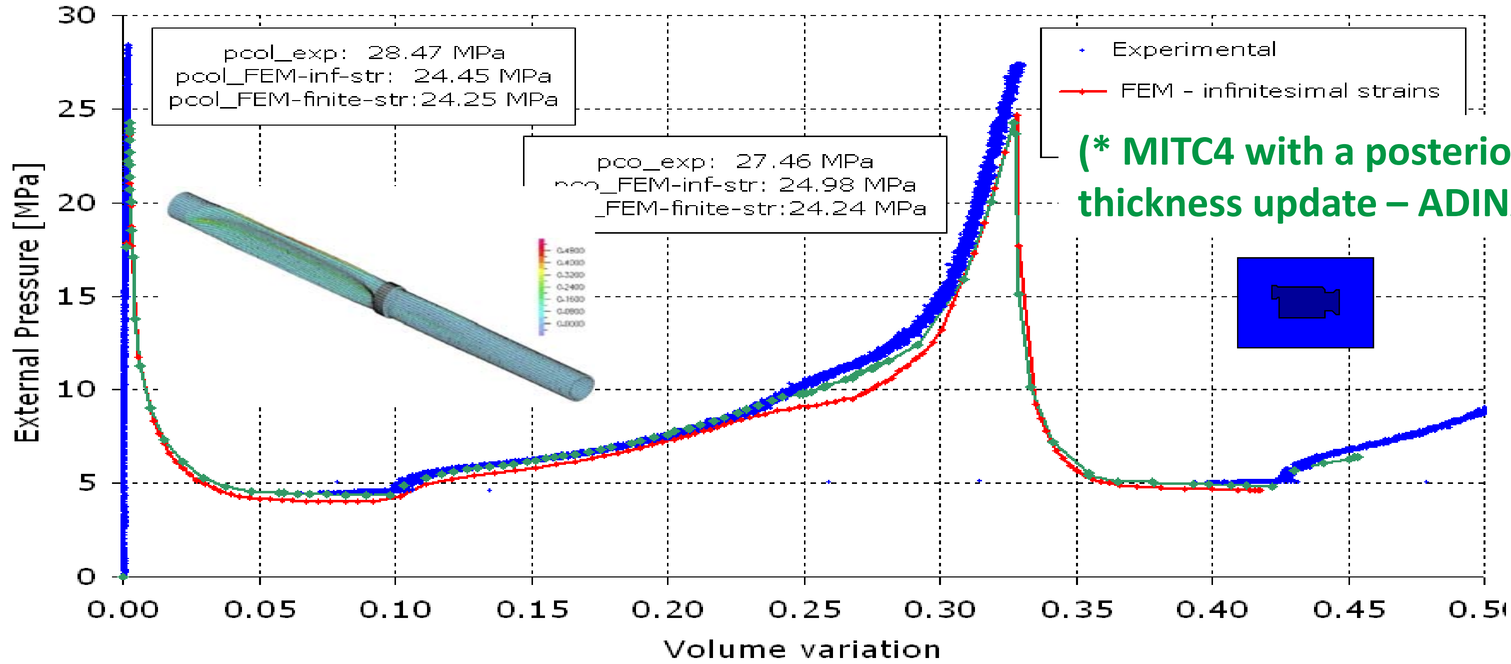

(* MITC4 with a posteriori thickness update – ADINA)

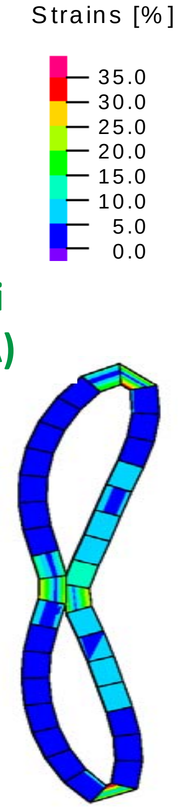

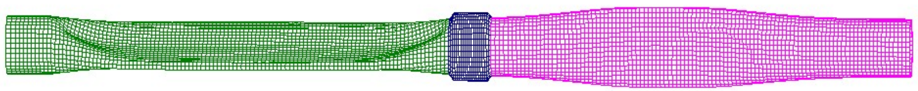

SIM&TEC
Simulación y Tecnología
Simulation and Technology

Validation: Numerical vs. Experimental Response

Sample	Collapse pressure: FEA_finite strain/lab	Crossover pressure: FEA_finite strain/lab.	Mode
1	0.924	1.004	Flattening
2	0.928	0.985	Flattening
3	0.951	0.926	Flipping
4	0.852	0.883	Flipping

The two collapse modes reported in the literature, the flattening and the flipping mode, were identified in our simulations.

The agreement between the finite element predictions and the laboratory observations, both for the collapse and cross-over pressure, is very good; hence, finite element models can be used as a reliable engineering tool to assess the performance of integral ring buckle arrestors for steel pipes.